AIP | Review of Scientific Instruments

Measurement of inkjet first-drop behavior using a high-speed camera

Kye-Si Kwon, Hyung-Seok Kim, and Moohyun Choi

Citation: Review of Scientific Instruments **87**, 035101 (2016); doi: 10.1063/1.4940934
View online: http://dx.doi.org/10.1063/1.4940934
View Table of Contents: http://scitation.aip.org/content/aip/journal/rsi/87/3?ver=pdfcov
Published by the AIP Publishing

Measurement of inkjet first-drop behavior using a high-speed camera

Kye-Si Kwon,[a] Hyung-Seok Kim, and Moohyun Choi
Department of Mechanical Engineering, Soonchunhyang University, 22, Soonchunhyang-Ro, Shinchang, Asan, Chungnam 336-745, South Korea

(Received 25 November 2015; accepted 15 January 2016; published online 2 March 2016)

Drop-on-demand inkjet printing has been used as a manufacturing tool for printed electronics, and it has several advantages since a droplet of an exact amount can be deposited on an exact location. Such technology requires positioning the inkjet head on the printing location without jetting, so a jetting pause (non-jetting) idle time is required. Nevertheless, the behavior of the first few drops after the non-jetting pause time is well known to be possibly different from that which occurs in the steady state. The abnormal behavior of the first few drops may result in serious problems regarding printing quality. Therefore, a proper evaluation of a first-droplet failure has become important for the inkjet industry. To this end, in this study, we propose the use of a high-speed camera to evaluate first-drop dissimilarity. For this purpose, the image acquisition frame rate was determined to be an integer multiple of the jetting frequency, and in this manner, we can directly compare the droplet locations of each drop in order to characterize the first-drop behavior. Finally, we evaluate the effect of a sub-driving voltage during the non-jetting pause time to effectively suppress the first-drop dissimilarity. © *2016 AIP Publishing LLC.* [http://dx.doi.org/10.1063/1.4940934]

I. INTRODUCTION

The applicability of inkjet technology has increased from its use in home printers towards implementation as manufacturing tools. Drop-on-demand inkjet printing presents advantages over continuous inkjet printing because an ink droplet of an exact amount can be placed on an exact location without the use of any droplet deflection device. Jetting from a drop-on-demand inkjet head is not continuous because there is a non-jetting period (pause time) during the relative movement of the head and substrate in order to deposit the droplet on the target location of the substrate. Moreover, the printed substrate needs to be unloaded, and a new substrate should be loaded for printing, especially for printed electronics applications. A camera can be used to view the substrate to identify the printing position in the substrate in order to align the substrate with respect to motion stage axes prior to printing. This may take a considerable amount of time, and jetting should not occur during preparation for printing. During the non-jetting period, the ink on the nozzle surface can dry, and consequently, the jetting behavior of the first few drops is likely to differ from that observed during steady-state jetting. The existence of this first-drop problem has been discussed in the literature,[1–5] and if a significantly abnormal jetting behavior is present, the printing quality can be affected accordingly. As a result, a proper measurement method should be developed to evaluate the jetting failure.

Jetting monitoring techniques based on piezo-self-sensing have been proposed to detect jetting failures from an inkjet head.[6–8] This method can be used to immediately detect jetting failures to identify the possible cause of a failure. This is an effective method that can be used to monitor the jetting behavior during the entire printing process without the use of any vision systems for droplet imaging. However, this method requires averaging the self-sensing signals in order to remove electrical noise, and as a result, the method may not be able to detect dissimilarity in the first few drops.

A drop visualization system with a strobe LED (light emitting diode) can be used to visualize the jetting behavior.[4,9,10] This method is useful because real-time monitoring is possible through the use of a CCD (charge-coupled device) camera. However, this method cannot measure the transient jet behavior of the first few drops because it uses a low frame-rate (~30 fps) CCD camera with a strobe light to obtain a frozen image.

In this study, a high-speed camera is used to measure the first-drop failure because this is an effective means to measure the transient droplet behavior. To the authors' knowledge, only a few articles have been published to address the measurement of first-drop dissimilarity, and Famili *et al.* were probably the first to discuss the measurement of first-drop dissimilarity using a high-speed camera.[11] In their work, a frame rate of 2800 fps (frame per second) was used to acquire one single image for each droplet that was generated with a jetting frequency of 2.8 kHz.[11] However, the use of the same frame rate as the jetting frequency may have drawbacks in which a delay in the starting trigger of the high-speed camera with respect to the jet signal should be optimal in order to capture the jetting image. Otherwise, the image is very likely to capture background only, missing the droplet in the image. Also, if there is a significant deviation in the jetting speed due to first-drop effects, the abnormal jetting behavior may not be captured when a single image per droplet is acquired. Nevertheless, the use of a low frame rate may have an advantage regarding the image resolution because the size of the image (number of pixels in the image) can be larger. In addition, doing so can be efficient

[a]Author to whom correspondence should be addressed. Electronic mail: kskwon@sch.ac.kr. Telephone: Int +82-41-530-1670. Fax: Int +82-41-530-1550. URL: http://inkjet.sch.ac.kr/.

from a computational point of view since the number of images can be reduced in order to investigate only the behavior of the first few drops. Therefore, the frame rate of the high-speed camera should be determined by considering this trade-off.

The jetting images acquired from the high-speed camera can be used to calculate the jetting performance, including the jet speed and the drop volume. In a previous study, the droplet volume of the transient jetting was discussed in order to explain the first-drop dissimilarity.[11] However, the exact measurements of the droplet volume may be difficult to conduct due to the limited image resolution, particularly, in the case of high-speed imaging. Also, the droplet volume can be subjected to the threshold value that is required for conversion to a binary image.[4] In this study, we mainly discuss the jetting speed in order to evaluate the first-drop behavior because this can be measured with improved accuracy.[4] The use of the jetting speed of the droplet is straightforward to evaluate the inkjet since it is related to the jettability and the accuracy of the droplet placement. In the previous work, the relative location of the droplet is used to understand the relative jetting speed, instead of the jetting speed,[11] since the jetting speed could not be measured due to the use of only one image per drop. Note that at least two droplet images per drop should be acquired in order to measure the jetting speed.[4] As a result, we used a 9 kfps acquisition in this study to measure the first-drop dissimilarity of a droplet jetted with a jetting frequency of 1 kHz. Since the image frame rate is an integer multiple of the jetting frequency, the first drop can be easily evaluated by means of the repeatability of the droplet location in the acquired image. Also, by using a higher frame rate than the jetting frequency, drop imaging is less dependent on the starting time of image acquisition of the high-speed camera and at least two jetting images can be taken per droplet to calculate jetting speed.

Many factors could affect the behavior of the first drops. The most common causes for this are probably the changes in the jetting properties of the ink due to an increase in viscosity or surface tension, which are related to the evaporation of ink on the nozzle surface. Jet failures due to evaporation are closely related to the non-jetting idle time (pause time), so it is important to understand the effects of the non-jetting idle time on the first-drop failures. In this study, we propose the use of high-speed camera imaging techniques to evaluate the first-droplet dissimilarity in relation to non-jetting idle time. To the author's knowledge, few papers have discussed the effect of the non-jetting time on first-drop jet failures. The characterization of effect that the non-jetting idle time has on the first drops can be useful to develop a jet failure prevention scheme. For example, pre-spitting schemes on a dummy printing area prior to actual printing can be optimized. Also, the method using a sub-voltage during the non-jetting period can be optimized to reduce the first-drop dissimilarity. The sub-voltage method can be useful in practice because it can minimize substrate contamination due to pre-spitting prior to actual printing.[12,13]

II. EXPERIMENTAL SETUP

Fig. 1 shows the schematic of the experimental setup used to measure the first-drop effects with a high-speed camera.

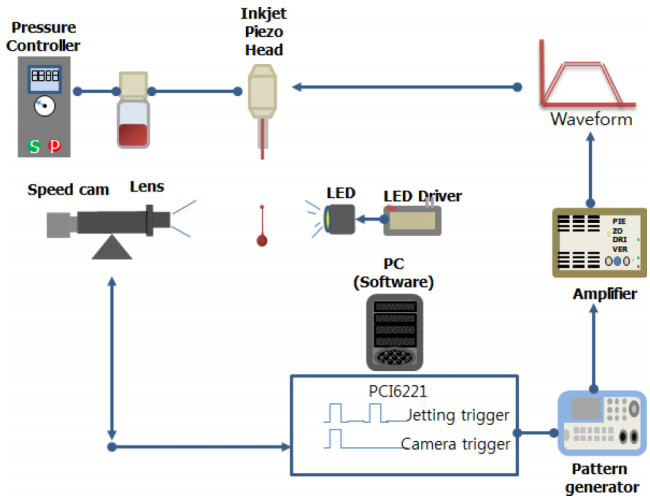

FIG. 1. Schematic of the experimental setup.

The jetting device consisted of a single nozzle head (MJ-AT, Microfab, USA) with a nozzle diameter of 50 μm for the printhead of this experiment. A slight negative pressure needs to be applied at the nozzle of the inkjet head because doing so can prevent dripping the ink from the nozzle. For this purpose, the meniscus pressure at the nozzle of the dispenser was controlled by the height of the ink reservoir. To maintain the proper meniscus pressure, the ink reservoir should sit slightly lower (about 2 cm) than the surface of the printhead nozzle so that the meniscus pressure at the nozzle can be slightly negative.

To obtain proper jetting, a trapezoidal driving waveform is used for jetting.[4] The rising/falling and dwell times of the waveform were set to 6 μs and 20 μs, respectively. The amplitude of the driving waveform was adjusted to obtain the target jetting speed. To simplify the analysis, a low jetting speed of 2–3 m/s was used since a low jetting speed produces fewer satellite droplets. Also, image blur due to droplet movement can be reduced by using a low jetting speed. Nevertheless, this method can be extended to higher jetting speeds without a loss of generality.

The same digital trigger signal is used for both the high-speed camera and the jetting driver in order to understand and measure the jetting images for the first few drops by simultaneously starting the image acquisition and jetting. Also, we used the steps described below to investigate the effect of non-jetting idle time, as shown in Fig. 2.

(1) Continuous jetting with sufficient time to ensure steady-state jetting.
(2) Jetting is stopped for a pre-determined non-jetting idle time, t_p. During the non-jetting period, both the high-speed camera and the jetting driver wait for the trigger to start jetting and for image acquisition.
(3) After the pre-determined pause time, the jetting and image acquisition will start simultaneously to measure the first-drop behavior.

The starting trigger after the pause time has been generated using digital I/O from a multi-function data acquisition I/O board (PCI-6221, NI, USA). The digital trigger can be used to start the digital pulse train from a counter in the

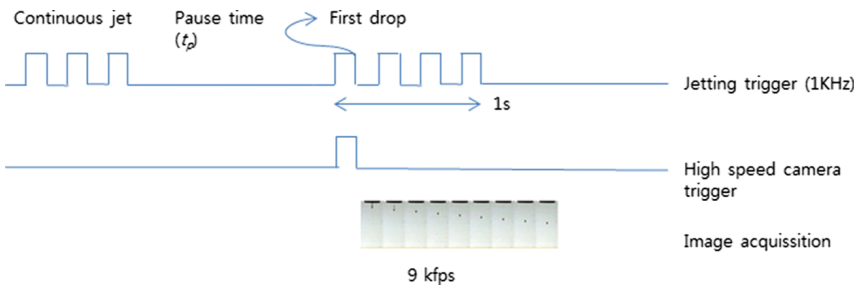

FIG. 2. Measurement schemes for the first-drop behavior with respect to the pause time.

PCI-6221 using a pre-determined frequency for ink jetting. Here, a jetting frequency of 1 kHz was used. At the same time as the starting trigger for jetting, the image acquisition is started with a frame rate of 9 kfps, which is 9 times higher than the jetting frequency. Note that the internal clocks for the jetting frequency and frame rate of the high-speed camera are independent in this experiment. As a result, there might be slight synchronization errors, even though we have used the same starting trigger for both devices. The magnitude of the synchronization errors and the effects on drop imaging will be discussed later.

It is important to set the frame rate to an integer multiple of the jetting frequency. As a result, the behavior of successive drops can be examined at the same time as jetting by inspecting every 9th frame. In particular, the first-drop behavior (transient drop behavior) can be evaluated by comparing the location of the droplet in every 9 images. If the behavior of the first few drops is different from the droplet image in steady-state jetting, then this could indicate that drying has occurred on the nozzle.

We used a high-speed camera (SpeedCam MiniVis, Weinberger, Switzerland) to capture the jetting images. The camera has an image resolution of 1280×1024 pixels at 500 fps, and the maximum recording speed is up to 112 000 fps. Note that the image resolution has been reduced as the frame rate increases. For example, in the case where images are acquired at 9 kfps, the number of pixels in the acquired image is 80×128, which is a very-low in resolution. The exposure time for the camera should be sufficiently short in order to avoid image blur due to droplet motion. However, a shorter exposure time results in dark images if the lighting is not sufficiently bright. In this study, we set the exposure time to 3 μs to take the lighting brightness into account. The effects of the illumination issues on the droplet images are further discussed in Ref. 5. After the acquisition of 1000 images at a frame rate of 9 kfps, the images are downloaded from the high-speed camera to the PC for further analysis.

III. EXPERIMENTAL RESULTS

Pure solvent may not block the nozzle because no solid content remains after evaporation. In this study, inks with different solid content were used in the experiment to demonstrate the effectiveness of the proposed measurement method for first-drop dissimilarity.

Several different jetting materials were used for the experiment, including a standard ink from Dimatix, nano-silver inks from ANP (DGP 40TE-20C, ANP, South Korea), and Harima (NPS-JL, Harima Chemicals, Japan).

A. Standard ink

Standard ink (XL-30, Dimatix, USA) was purchased from Fujifilm Dimatix. The viscosity of the model fluid was measured to be 14 cP at 25 °C.[7] The model fluid shows less evaporation on the nozzle surface because it is intended for use in inkjet head tests. As a result, nozzle clogging problems may not be likely to be as severe as with other functional inkjet inks.

Fig. 3 shows a high-speed camera image of the first few drops of standard ink after a non-jetting idle time of t_p = 540 s. As shown in Fig. 3, first-drop problems are not as severe when compared to the steady state. Since the frame rate is 9 times higher than the jet frequency, the same timing for each droplet is repeated every 9 frames. As a result, almost the same droplet location is observed every 9 frames when jetting at close to steady-state conditions, as shown in Fig. 3. Note that the droplet location is slightly closer to the nozzle for the first drop d = 1 when compared to other drops d = 2,

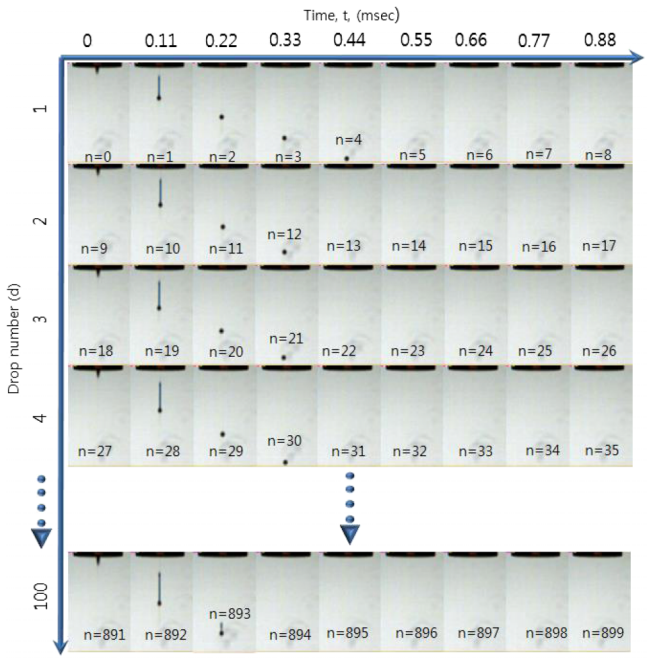

FIG. 3. High-speed camera image of standard ink with a non-jetting time of 540 s.

3, . . . , which indicates a slightly slower jetting speed for the first droplet compared to the other droplets.

For easier image analysis, the frame number of images, $n = 0, 1, 2, \ldots, 999$, in sequential order can be converted to drop number, d, and time, t, from jetting signal as

$$\begin{aligned} d &= \text{Quotient}\,(n/r) + 1, \\ t &= \text{Remainder}\,(n/r)/\text{frame rate} \\ &\approx \text{Remainder}\,(n/r)^{*}0.11\ \text{ms}, \end{aligned} \tag{1}$$

where r is the integer 9, which corresponds to a camera frame rate divided by the jetting frequency.

By using Equation (1), images can be effectively sorted with respect to the drop number d and time t from frame number n. The frame number is in the sequential order of the image acquisition. For example, the frame numbers for the starting time of each droplet, that is $t = 0$ s, can be sorted as n = 0, 9, 18, . . . , which correspond to drop numbers of $d = 1, 2, 3, \ldots$, respectively.

Fig. 4 shows the droplet location sorted with respect to the drop number, $d = 1, 2, 3, \ldots$, (horizontal axis) and time (vertical axis). By comparing droplet locations at a specific time, we can decide the drop number required beyond which jetting is similar to steady-state jetting. The leading edge of the droplet can be overlaid to compare the droplet locations, as shown in Fig. 4 (at t = 0.22 ms). In this example, only a few initial jettings were sufficient to ensure that jetting was similar to that of steady state jetting with regard to the droplet locations. The requirement for an acceptable jetting condition can differ according to the application, and in this study, we assume that the deviation in jetting speeds and locations within 20% that of the steady state are acceptable.

The droplet behavior is effectively analyzed using software developed to read and analyze the images. For this purpose, each image has been analyzed using a particle analysis technique based on a binary image in order to find the location of the droplet within the image. For the image analysis, NI Vision Assistant Module (NI, USA) is used to automate the measurements. The author's recent book[14] can be used as reference for further details.

The particle analysis algorithm is used to plot the droplet locations (vertical axis) with respect to the drop number (horizontal axis), as shown in Fig. 5. In this manner, the efforts for the image analysis can be reduced through automation when a large number of images need to be analyzed. Also, the jetting speed can be easily calculated according to the droplet locations. An explanatory video can be found from the website in Ref. 15 for better understanding.

The jetting speed of a specific drop number d can be calculated by using the droplet locations of two timings at $t_1 = 0.11$ ms and $t_2 = 0.22$ ms.

From the two images, the bottom locations, P_{y2} and P_{y1}, at two timings, t_2 and t_1, respectively, are used to calculate the jetting speed, V, as[4]

$$V = \frac{P_{y2} - P_{y1}}{t_2 - t_1}. \tag{2}$$

In this study, the jetting speed is effectively calculated from the identified locations by using the laboratory-developed image processing software shown in Fig. 5. Note that the starting time for the camera imaging is likely to vary slightly with respect to the jetting start time even though the same digital trigger signal is used for both image acquisition and jetting. This is a result of using independent internal clocks for the inkjet driver electronics for jetting and the high-speed camera. In such cases, the jetting speed can have an advantage over the droplet location for direct comparison because it is affected less by slight variations in the starting time of image acquisition. Also, the jettability after the non-jetting pause time can be easily understood via measurements of the jetting speed for the first few droplets.

Fig. 6 shows the variation in jetting speed (vertical axis) with respect to the drop number (horizontal axis) and the pause time t_d. As shown in the figure, the first-drop dissimilarity is not significant, and only a few drops are required to reach about 80% of the steady-state jetting speed for both the non-jetting

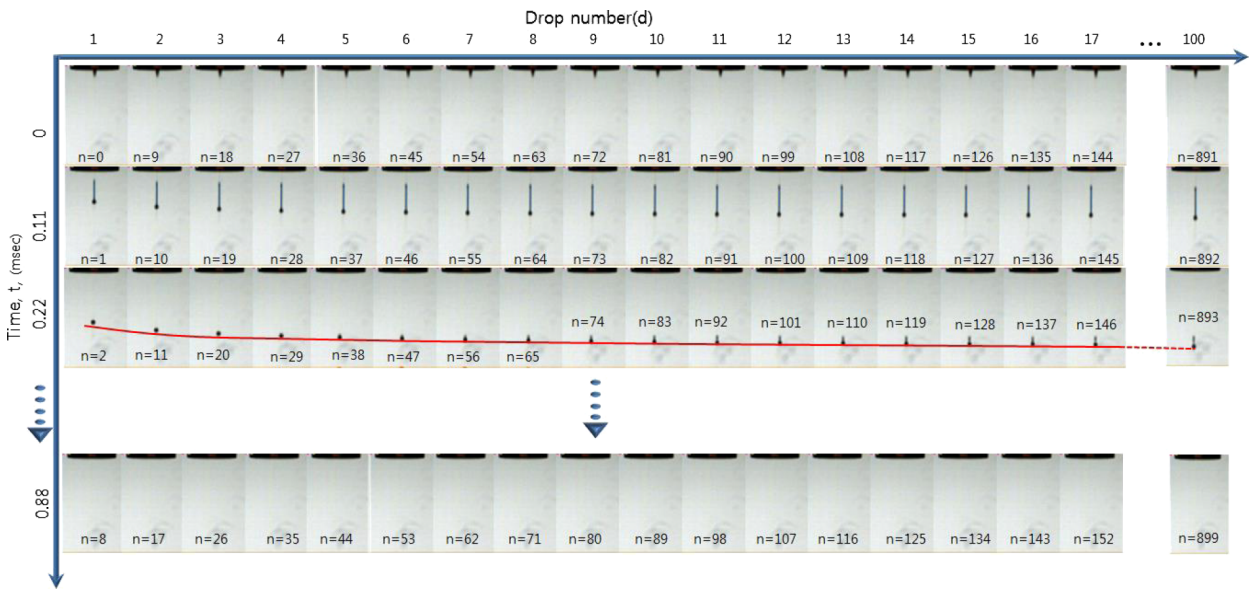

FIG. 4. Droplet locations for standard ink with respect to the drop number and time for $t_p = 540$ s.

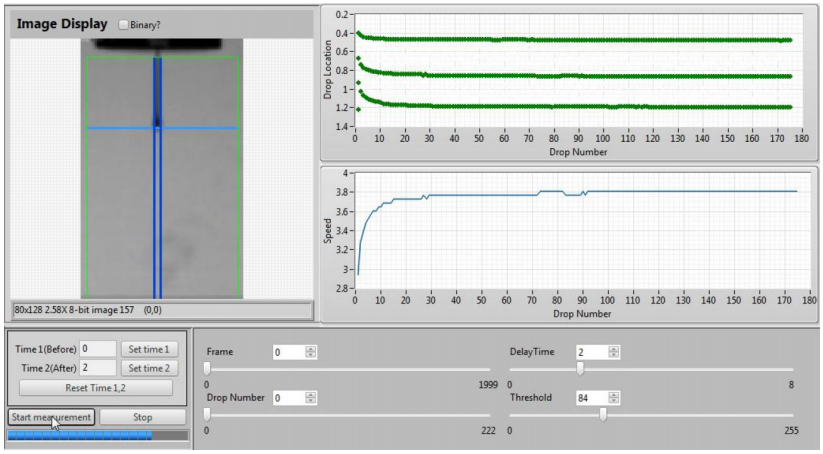

FIG. 5. Image analysis software for droplet locations with respect to the drop number. (Multimedia view) [URL: http://dx.doi.org/10.1063/1.4940934.1]

pause times of 60 s and 540 s. Note that the jetting speed of the first few drops becomes slower when the non-jetting idle time has increased. Also, more droplets must be released for the droplets to acquire the speed of the steady-state droplets.

B. Silver ink

1. Silver ink from ANP

Silver ink from ANP (Silverjet, DGP-40TE-20C, ANP, South Korea) was used as a jetting material in order to investigate the effects of the non-jetting idle time. The ink has a Ag particle content of 30 wt. %, and the main solvent is TGME (Triethylene Glycol Monoethyl Ether, $C_8H_{18}O_4$). The viscosity of the ink is 7.8 cP at 25 °C. For this purpose, 6 sets of jetting images are acquired by using a range of non-jetting pause times of t_p = 0, 60, 180, 300, 420, and 540 s. For direct comparison, the jetting images of each first drop d = 1 are compared, as shown in Fig. 7.

Fig. 7 clearly shows that an increase in the pause time (vertical axis), t_p, results in a slower jetting speed than that at the steady state with t_p = 0. Note that a droplet location closer to the nozzle indicates a low jetting speed, which is contrary to that observed in a previous publication[11] that presented experimental result of a faster jetting speed for the first drop when compared to that of steady-state jetting.

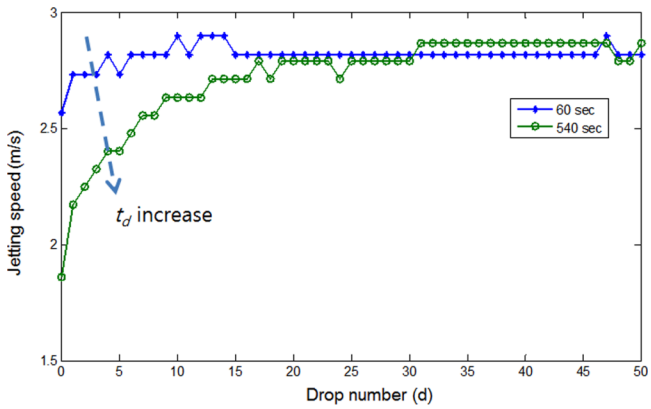

FIG. 6. Jetting speed plot for standard ink with respect to the drop number and non-jetting pause times of t_d = 60 s and 540 s.

It is well known that it takes time for ink to extrude from the nozzle because the propagation of a pressure wave of ink is required inside of the inkjet head. In the case of a Microfab head, it normally takes more than about 40 μs for ink extrusion due to the driving voltage length (about 30 μs) and the ink pressure wave propagation time. As a result, we cannot observe droplet extrusion at the time of jetting triggering at t = 0. Nevertheless, we observed a slight droplet extrusion for t_p = 0 s and 540 s at t = 0, i.e., n = 0, which indicates that the starting time of the image acquisition may have a slight delay of up to 50 μs with respect to the jetting trigger. This is related to synchronization errors because two different internal clocks are used to start both the jetting and imaging acquisitions. Nevertheless, the magnitude of the error is acceptable to conduct an analysis of the first drop behavior.

As shown in Fig. 7, the droplet location in the image for an idle time of t_p = 60 s was not significantly different from that

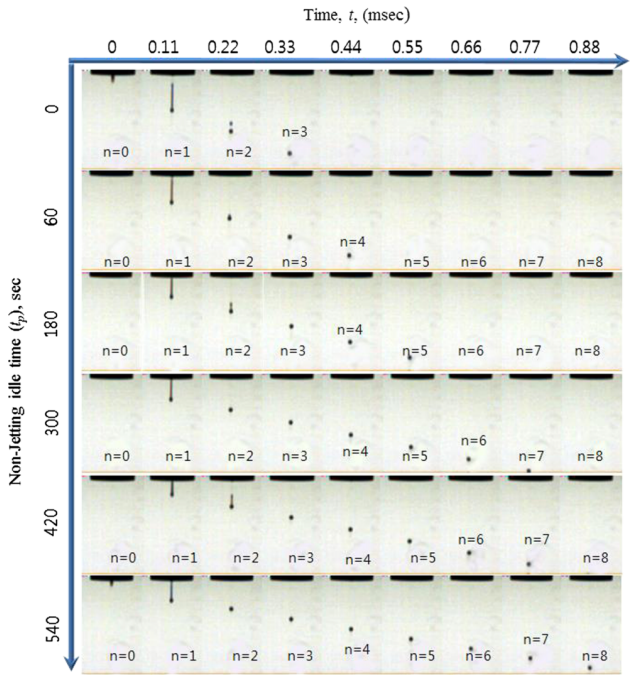

FIG. 7. Effects of the non-jetting pause time on the first-drop behavior of the ANP silver ink.

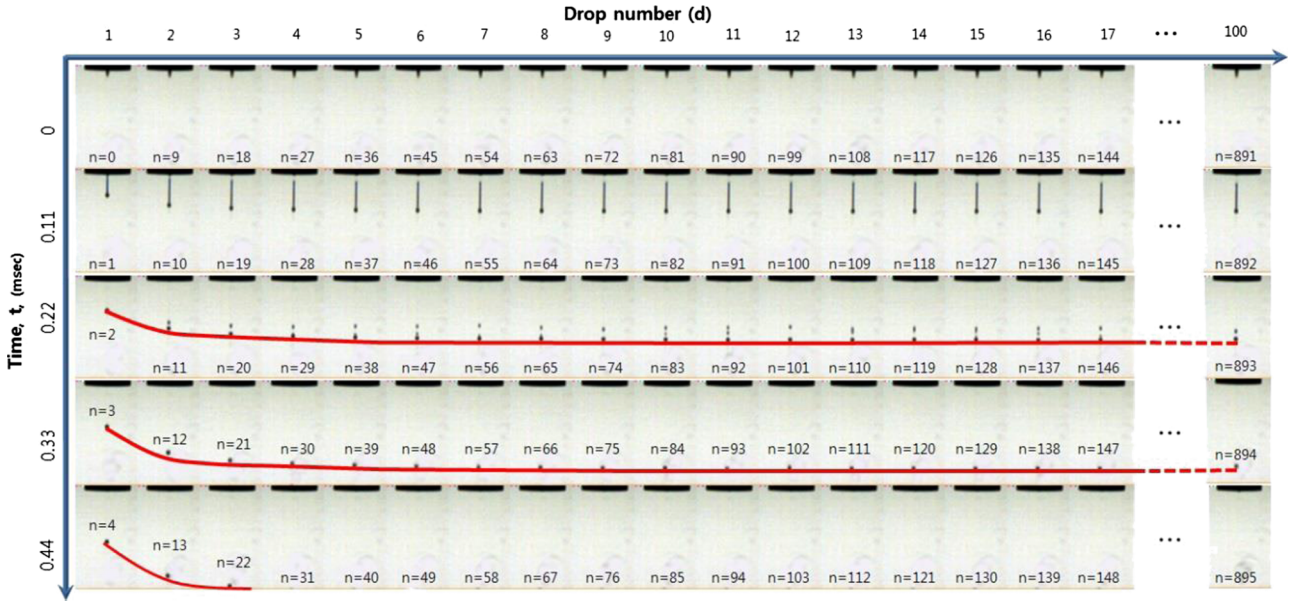

FIG. 8. Jetting image plot of the ANP silver ink of $t_p = 540$ s with respect to the drop number d and time t.

of the steady state, $t_p = 0$. As a result, the placement error from the first droplet may be negligible in the case of $t_p = 60$ s. We also observed that first-droplet jetting was possible even if the pause time had increased up to $t_p = 540$ s, which is acceptable for most printing applications. However, the jetting speed was very slow with $t_d = 540$ s when compared to that of the steady state case. This slow jetting speed is likely to be alleviated after a few drops of jetting, and the number of droplets required to recover the jetting status may differ according to the ink used and other jetting conditions. To provide a better understanding, we take the example of the jetting images for a pause time of $t_p = 540$ s. For this purpose, the jetting images are sorted according to the drop number (horizontal axis) d and time (vertical axis) t, as shown in Fig. 8. The sorting method based on the sequential frame images, n, is discussed in Equation (1).

Fig. 8 shows that for the first drop $d = 1$, the drop locations (first column) are significantly different from those of other drops (other columns, $d = 2,3,4,\ldots$). It is clear in the jetting images that jetting recovered quickly within 2-3 drops, and the bottom-of-droplet locations are overlaid using a red line to conduct a comparison of the droplet locations for each droplet. In this manner, we can easily judge the jetting status by the straightness of the overlaid line. If the locations of the droplets do not change (straight line), then we can assume that jetting has achieved steady-state status. As shown in the figure, only a few drops prior to actual printing are required to produce steady-state jetting, even when the non-jetting idle time is as long as 540 s.

Alternatively, the jetting speed plot with respect to drop number n and pause time t_p can be used to evaluate the jettability after various trial pause times.

As shown in Fig. 9, only a few drops are required to reach 80% of the steady-state jetting for all $t_p = 60$, 300, and 540 s. Note that the number of droplets required for steady-state jetting may not be directly proportional to the non-jetting idle time, as shown in Fig. 9. The use of the jetting speed graph with respect to the drop number has advantages over sorted jetting images in which it is easier to conduct direct comparisons of many different conditions. However, it should be noted that the jetting speed is difficult to calculate when many droplets are present on the image, such as with a droplet image containing many satellites or a high-frequency jetting image.[16]

2. Silver ink from Harima

In this section, silver ink (NPS-JL, Harima Chemicals, Japan) is used as the jetting material in order to investigate the first-drop dissimilarity. The main solvent for the ink consists of n-tetradecane. The viscosity of the ink is 11 cP at 25 °C. Silver ink from Harima has a greater metal content of 55 wt. % when compared to ANP ink of 30 wt. %. With an increase in the solid content, first-drop jetting is more likely to be affected by the non-jetting idle time. Therefore, a trade-off between jetting reliability and material functionality should be considered when the inkjet ink is selected.

Fig. 10 shows the jetting image plot for the first drop $d = 1$ with respect to the non-jetting idle times.

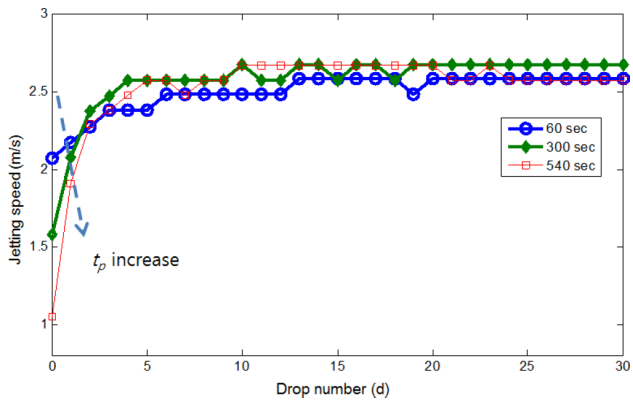

FIG. 9. Jetting speed plot of the ANP silver ink with respect to drop number and non-jetting idle time.

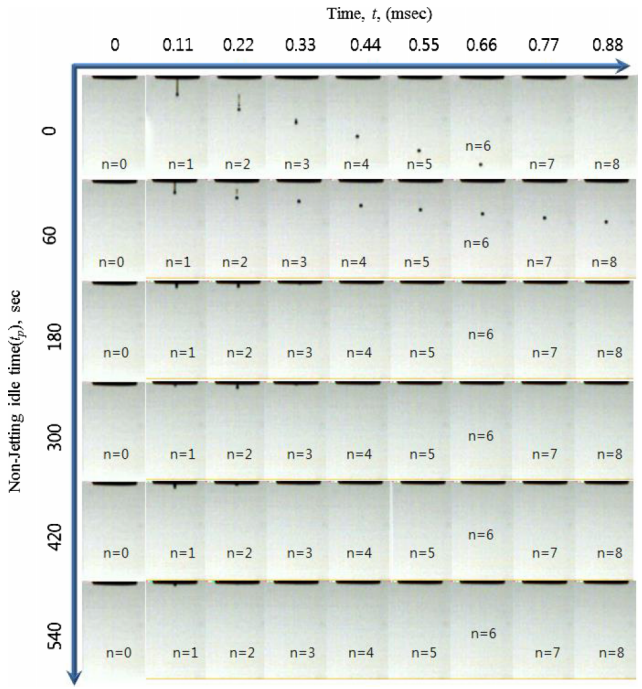

FIG. 10. First-drop jetting image plot for Harima ink with respect to different non-jetting idle times.

As shown in Fig. 10, the first-drop behavior is significantly affected by the non-jetting idle time, t_p (vertical axis). It is obvious that the first-drop jetting behavior is aggravated as the non-jetting time increases. Note that there was no jetting for the first few driving voltage pulses with a pause time exceeding 180 s.

To better understand the jetting behavior of the first few drops, the jetting images with a pause time of 60 s are sorted according to the drop number d and the time from the jetting trigger t, as shown in Fig. 11. In that figure, we can clearly observe a slower jetting speed in the first few drops. For example, in the case of a droplet image for the 2nd and 3rd drops ($d = 2$ and $d = 3$), the previous 1st and 2nd drops still appeared in the image because the travel distance in the previous drop was very short during the jetting period (1 ms) since a very slow jetting speed was obtained for the first few drops. As a result, the accuracy of the drop position will be very poor when using the first few drops for printing. The effect of the variation in the jetting speed on the printing placement error is discussed in Ref. 9. Note that the possible placement errors for the first few drops can be prevented by pre-spitting prior to actual jetting, and the number of pre-spits can be determined by using our measurement method. For example, it can be easily understood that 4 drops, $d = 4$, are required for the drop location to reach more than 80% that of the steady-state location.

To investigate the case where the first few driving voltage pulses do not produce jetting, jetting images for a pause time of $t_p = 180$ s are sorted according to the drop number (horizontal axis) and time (vertical axis) as shown in Fig. 12. There was no jetting up to 4 driving voltage pulses $d = 4$, and the non-jetting conditions due to nozzle blockage could result in critical printing failures with missing dots on targeted locations. However, once we understand the jetting behavior of the initial stage, failures can be effectively prevented. The non-jetting condition can be returned to a jetting condition with a few driving voltage pulses (pre-spitting), which may remove the dried part of the ink on the nozzle surface through meniscus excitation. The number of excitations required (driving voltage pulses) to lead to jetting depends on the degree of changes in the ink properties. Note that jetting speed for the first droplet after a few non-jetting driving voltage pulses is likely to be very slow, as shown in Fig. 12. Therefore, several more jettings are required to reach steady-state jetting conditions. For example, we can easily understand from Fig. 12 that additional 10 jetting drops are required to achieve steady-state jetting after the first appearance of a jetted drop. In total, about 14 jetting driving pulses, $d = 14$, are required to ensure proper printing after a pause time of 180 s. In this

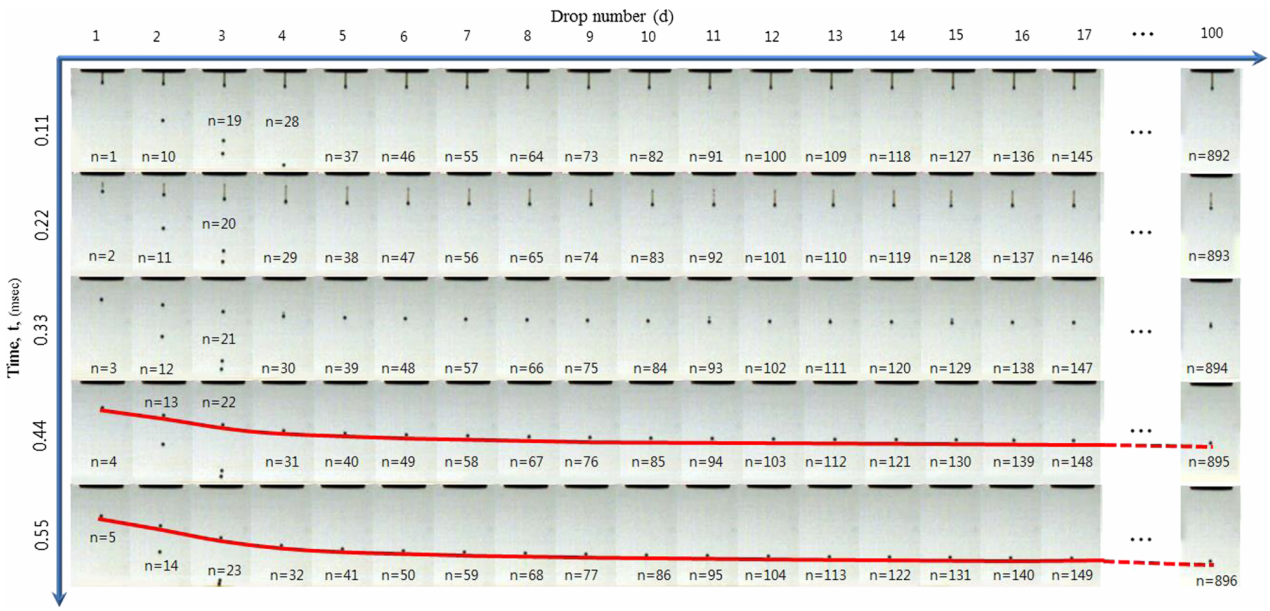

FIG. 11. Jetting image plot of Harima silver ink with $t_p = 60$ s.

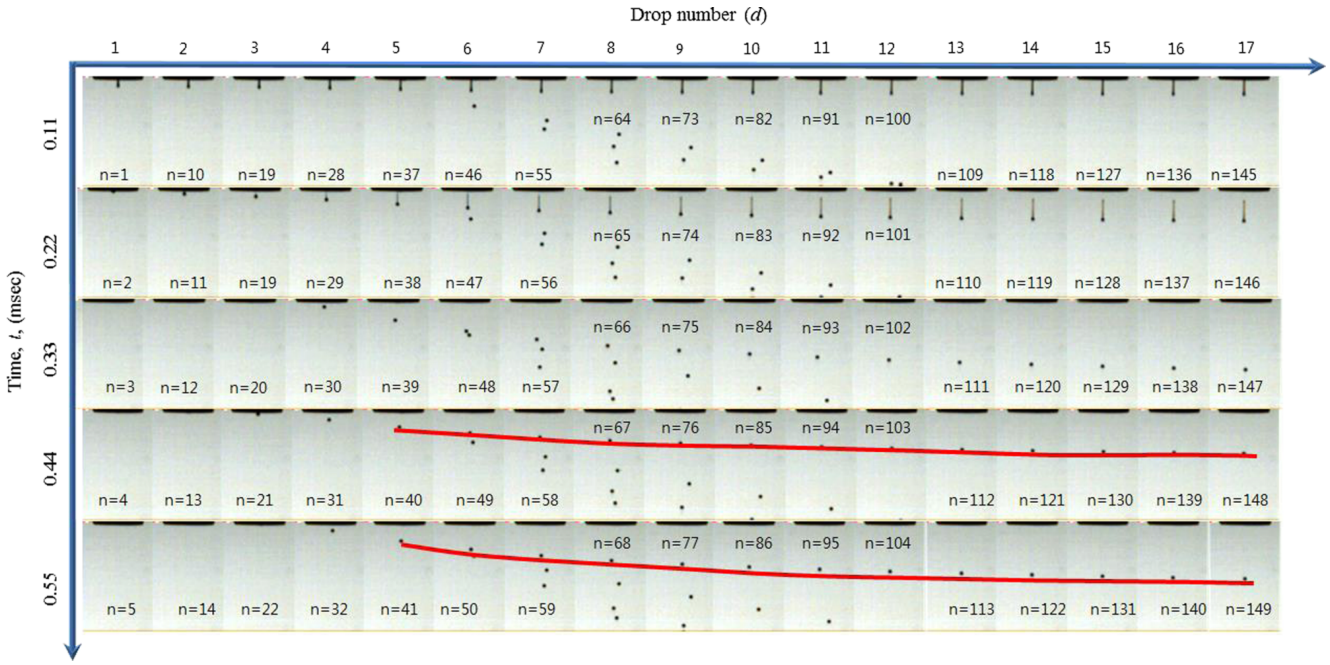

FIG. 12. Jetting image plot of Harima silver ink with t_p = 180 s.

manner, our measurement of first-drop behavior can be used to determine the pre-jetting number in order to prevent jetting failures resulting from non-jetting idle time.

It is obvious that the first-drop effect is aggravated when the non-jetting time increases. Eventually, the nozzle blockage condition cannot be returned to a normal jetting condition with the excitation voltage alone. For example, in the case of t_p = 480 s, the nozzle blockage could not be removed using the driving voltage only. Consequently, maintenance schemes including purge and wiping are required to recover to a normal jetting condition. This maintenance process is complicated, and a large quantity of ink can be wasted during maintenance. Therefore, it is important to keep the nozzle ready for jetting without clogging. When the head is required to be idle for a long time, we recommend that a few droplets be jetted at every pre-determined time interval. The proposed measurement method can be used to decide the number of pre-spitting droplets required and the time interval, which can ensure the printing quality and jetting reliability.

Although the pre-spitting method prior to actual printing is an effective means to avoid abnormal jetting for the first few drops and to maintain the jetting condition, it can also result in contamination on the substrate. To avoid substrate contamination, the print head should be moved to a designated location for pre-spitting, and therefore, the printing process is further complicated.

As an alternative to pre-spitting, the use of a low voltage excitation during the non-jetting idle time can reduce nozzle clogging on the nozzle surface through an excitation of the meniscus.[12,13] The author's previous work showed that the meniscus of the inkjet nozzle can be effectively excited without actual jetting when a low driving voltage is applied.[17]

To excite the meniscus without jetting, a waveform voltage of 28 V was applied during the non-jetting idle time. Note that a 38 V waveform was used for jetting.

Fig. 13 shows the jetting images for the first drops when the sub-voltage is applied during non-jetting idle times of t_p = 0, 60, 300, and 540 s. Here, t_p = 0 indicates steady-state jetting. When compared to the droplet images without a sub-voltage shown in Fig. 10, the jetting condition can be maintained for a considerable non-jetting period. For example, the first driving voltage d = 1 can produce a jetted droplet at up to t_p = 540 s, which is acceptable for most practical applications. To provide a better understanding, Fig. 14 shows jetting images for an idle time of t_p = 540 s, sorted with respect to drop number d and time t. As shown in the figure, the use of the sub-voltage has advantages due to the abnormality in the first few jettings that can be significantly reduced without actual jetting. However, it should be noted that the sub-voltage should be considered to be a supplementary method to

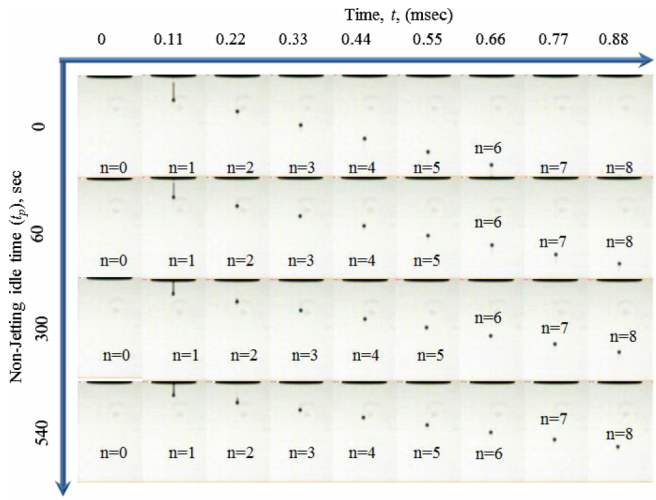

FIG. 13. Jetting images of Harima silver ink with sub-voltage when t_p = 540 s is used.

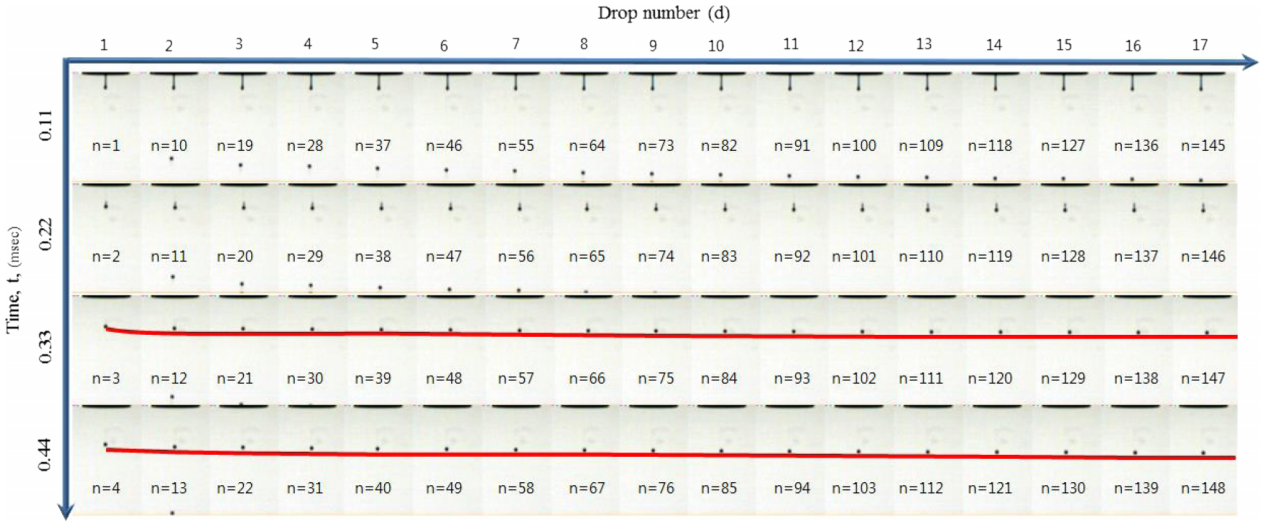

FIG. 14. Jetting behavior of Harima silver ink using a sub-voltage during the non-jetting time of $t_d = 540$ s.

maintain jetting conditions. The combination of a few periodic jettings and a sub-voltage during the non-jetting periods is recommended in order to maintain the jetting conditions for long non-jetting pause times.

IV. DISCUSSION AND CONCLUSION

The first-drop dissimilarity is evaluated using a proposed method based on high-speed camera imaging. To effectively understand the jetting behavior, we set the frame rate of the high-speed camera to 9 kfps, which is an integer multiple of the jetting frequency of 1 kHz. In this manner, the effect of the first-drop can be effectively understood by conducting a comparison of droplet images sorted according to drop number and time because the droplets viewed once every 9 images will have occurred at the same time from jetting. This method is not limited to a specific jetting frequency and camera frame rate since the proposed method can be extended for use in any cases where the image frame rate is an integer multiple of the jetting frequency.

We have observed that the jetting speed of the first drop slowed down as the non-jetting pause time increased, which is contrary to what was previously found by another group. The inkjet head was shown to develop non-jetting conditions as the non-jetting period is increased with the jetting speed tending toward zero. To minimize the degree of the first-drop dissimilarity after a given non-jetting idle time, we propose the use of a required number of jetting driving voltage pulses to recover the jetting status. This can be achieved simply through pre-spitting prior to printing, and the number of drops required for jetting status recovery can be jetted on a dummy area prior to printing to ensure better printing quality. However, the number of pre-spittings prior to printing should be minimized in order to avoid substrate contamination and to reduce wasted ink. To minimize pre-spitting, a sub-voltage pulse applied during the non-jetting idle time was shown to be effective. The experimental results with Harima silver ink indicate that first-drop jetting was possible even with an idle time of 540 s by using the proposed sub-voltage during the non-jetting time, whereas the nozzle is completed clogged when the sub-voltage is not applied. Also, the jetting condition easily returns to normal with a few jetting drops if the sub-voltage is used for meniscus excitation. Based on our experimental results, we recommend that a combination of pre-spitting and sub-voltages during non-jetting idle time should be used to keep nozzle status jettable for a long period of time.

ACKNOWLEDGMENTS

This work was supported by the Mid-career Research Program through a NRF grant funded by MEST (No. NRF-2013R1A2A2A01004802) and was also partially supported by the Soonchunhyang University Research Fund.

[1]P. Calvert, "Inkjet printing for materials and devices," Chem. Mater. **13**, 3299–3305 (2001).
[2]H. Dong, W. W. Carr, and J. F. Morris, "Visualization of drop-on-demand inkjet: Drop formation and deposition," Rev. Sci. Instrum. **77**, 085101 (2006).
[3]R. M. Verkouteren and J. R. Verkouteren, "Inkjet metrology. II: Resolved effects of ejection frequency, fluidic pressure, and droplet number on reproducible drop-on-demand dispensing," Langmuir **27**(15), 9644–9653 (2011).
[4]K. S. Kwon, in *Vision Monitoring in Inkjet-Based Micromanufacturing*, edited by J. G. Korvink, P. J. Smith, and D.-Y. Shin (Wiley-VCH Verlag GmbH & Co. KGaA, Weinheim, Germany, 2012).
[5]J. F. Dijksman, P. C. Duineveld, M. J. J. Hack, A. Pierik, J. Rensen, J. E. Rubingh, I. Schram, and M. M. Vernhout, "Precision ink jet printing of polymer light emitting displays," J. Mater. Chem. **17**(6), 511–522 (2007).
[6]K. S. Kwon, Y. S. Choi, D. Y. Lee, J. S. Kim, and D. S. Kim, "Low-cost and high speed monitoring system for multi-nozzle inkjet head," Sens. Actuators, A **180**, 154–165 (2012).
[7]K. S. Kwon, Y. S. Choi, and J. K. Go, "Inkjet failures and their detection using piezo self-sensing," Sens. Actuators, A **201**, 335–341 (2013).
[8]M. A. Gronninger, P. G. M. Kruijt, H. Reinten, R. H. Schippers, and J. M. M. Simons, "A method of controlling an inkjet printhead, an inkjet printhead suitable for use of said method, and an inkjet printer comprising said printhead," European patent, EP 1378360 A1 (2003).
[9]K. S. Kwon, "Experimental analysis of waveform effects on satellite and ligament behavior via in situ measurement of the drop-on-demand drop formation curve and the instantaneous jetting speed curve," J. Micromech. Microeng. **20**, 115005 (2010).
[10]K. S. Kwon, D. Zhang, and H. S. Go, "Jetting frequency and evaporation effects on the measurement accuracy of inkjet droplet amount," J. Imaging Sci. Technol. **59**(1), 020401 (2015).

[11]A. Famili, S. A. Palkar, and W. J. Baldy, Jr., "First drop dissimilarity in drop-on-demand inkjet devices," Phys. Fluids **23**, 012109 (2011).
[12]W. J. Baldy, Jr., A. Famili, and S. A. Palkar, "Sub-threshold voltage priming of inkjet devices to minimize first drop dissimilarity in drop on demand mode," European patent, EP 2418085 A1 20120215 (2012).
[13]W. Voit, I. Reinhold, W. Zapka, L. Belova, and K. V. Rao, "Utilization of industrial inkjet technologies for the deposition of conductive polymers, functional oxides and CNTs," in *MRS Spring Meeting* (Material Research Society (MRS), 2011), Vol. 1340.
[14]K. S. Kwon and S. Ready, *Practical Guide to Machine Vision Software: An Introduction with LabVIEW* (Wiley, 2015).
[15]K. S. Kwon, "Image analysis software for droplet locations," available at online: https://youtu.be/rP-6ER3x358.
[16]K. S. Kwon, M. H. Jang, H. Y. Park, and H. S. Ko, "An inkjet vision measurement technique for high frequency jetting," Rev. Sci. Instrum. **85**, 065101 (2014).
[17]K. S. Kwon, "Waveform design methods for piezo inkjet dispensers based on measured meniscus motion," IEEE/ASME J. Microelectromech. Syst. **18**(5), 1118–1125 (2009).